# Multiple Interaction Regions in the Orthosteric Ligand Binding Domain of the α7 Neuronal Nicotinic Acetylcholine Receptor

Yunde Xiao,* Philip S. Hammond, Anatoly A. Mazurov, and Daniel Yohannes

Targacept, Inc., 200 East First Street, Suite 300, Winston-Salem, North Carolina 27101, United States

ABSTRACT: Neuronal nicotinic receptors (nAChRs) belong to the Cys-loop family of ligand-gated ion channels and are formed from five subunits either as homologous or heterologous, oligomeric receptors, and are of interest as targets for treatment of a variety of central and peripheral nervous system disorders. Using a model of the homopentameric α7 nAChR extracellular region derived from the homologous acetylcholine binding protein (AChBP) from *Aplysia* California, binding modes of structurally diverse, high affinity α7 ligands were examined by docking to the orthosteric

ligand binding domain. While all α7 ligands show similar interactions between the essential positively charged cationic center of the ligand and αTRP147 of the receptor (i.e., hydrogen bond to the tryptophan backbone carbonyl and cation-π interaction), docked poses of various ligands show the potential to interact with three additional regions within the binding domain, identified as regions 1, 2, and 3. Region 1 is located in the vicinity of Loop-E, involves ligand–protein interactions via a network of water-mediated hydrogen bonds, and is analogous to the region where pyridinyl groups are located in many of the AChBP-nicotinic ligand cocrystal structures. Ligands interacting with region 2 probe an area that spans from Loop-E to Loops-D and -F and may contribute to α7-selectivity over other nAChR subtypes. Several high affinity α7 ligands show strong interactions in this region. Region 3 is located near Loop-F of the protein and is analogous to an area involved in binding of an active metabolite derived from DMXBA, in an AChBP cocrystal structure. It appears that π–π interactions contribute to binding affinities of α7 nAChR ligands in this latter region, and further, this region may also contribute to α7-selectivity over other nAChR subtypes. Analysis of the resulting poses suggests that compounds with high α7 binding affinity do not require interactions across all regions simultaneously, but that interactions in multiple regions may enhance ligand binding and increase selectivity. Our results provide insight for further development of selective α7 nAChR ligands and may prove useful for the design of novel scaffolds for specific nicotinic therapeutic agents.
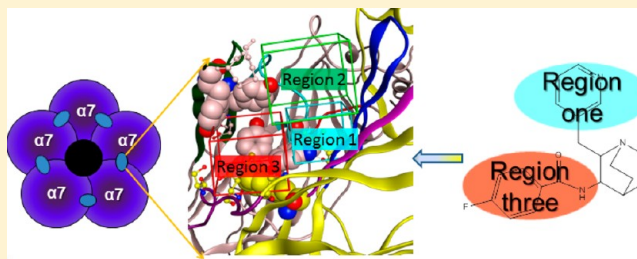
■ INTRODUCTION

Neuronal nicotinic acetylcholine receptors (nAChRs) are members of the Cys-loop ligand gated ion channels (LGIC) superfamily found in the central and peripheral nervous systems that regulate synaptic and extrasynaptic activity.[1−3] nAChRs are considered as a viable drug target since nAChR subtypes modulate key neurotransmitter and regulatory pathways associated with various diseases, including Alzheimer's, Parkinson's, and schizophrenia, are a validated target for cessation of smoking, and have been studied for pain management.[4] Several nicotinic receptors ligands are under investigation as clinical targets.[5] Varenicline, a partial agonist at α4β2 and a full agonist at α7 nAChRs, is currently in use for smoking cessation[6] and is under clinical investigation for use against depression and Parkinson's as well as cognitive deficits in schizophrenia.

Various studies combining genetic, protein, immunological, microscopic, and functional assays reveal that each nAChR structure consists of five protein subunits.[7] A number of nAChR subtypes are known to exist and arise from differential association of these various subunits. However, all nAChR subtypes share a common structural motif: they are homo- or heteropentameric ligand-gated ion channels. The orthosteric

binding site for the endogenous neurotransmitter, acetylcholine, lies at the interface between adjacent subunits, i.e. two identical subunits in the case of homomeric receptors and between differing subunits in the case of heteromeric receptors. Thus, homopentameric receptors have five acetylcholine binding sites while heteropentameric receptors have two primary sites as well as an additional site that contributes to isoform-specific agonist sensitivity.[8] In all cases, the principal side of the ligand binding site is produced by an α-type subunit, which provides unique contributions to the kinetics of channel gating and ligand binding. The complementary face is produced by an α-type or other-type subunit and is involved in ligand selectivity.[9]

Structural information on nAChRs is limited since these receptors are large membrane proteins that are difficult to crystallize for X-ray diffraction or have broadened NMR spectral resonance peaks. However, through electron microscopic studies, Unwin provided structural information on a heteromeric muscle-type nAChR at 4 Å resolution[10] which revealed features of the nAChR main chain and positions of

Table 1. Binding Affinities of Nicotinic Ligands

Structure	Name	Reference	Human α7 Ki (nM)[a]	Human α4β2 Ki (nM)[b]
	GTS-21/DMXBA	25	1200±444.6	51±17.0
	AR-R-17779	26	400±129.4	>5000
	Epibatidine	27	16±13.4	0.25±0.22
	TC-CMP01	28	340±191.4	670±731.0
	4-OH-GTS-21	29	1200±288.9	19±12.2
	TC-CMP02	30	60±34.4	>5000
	TC-CMP03	30	270±81.8	>5000
	Varenicline	31	290±76.9	0.14±0.07
	SSR180711A	32	17	>5000
	PNU-282987	33	27[c]	>5000
	TC-7020	34	3±4.7	1200±653
	AZD0328	35	22±12.1	52±24.8
	SEN12333 / WAY317538	36	290	>5000

[a] α7 radioligand [³H]-methyllycaconitine binding was determined in HEK human α7 membranes using standard methods as described in previously.[37] [b] the nicotinic radioligand [³H]-epibatidine binding to α4β2 nAChRs in human SH-EP1 cell membranes was assayed using standard methods adapted from published procedures.[38] [c] PNU-282987 displaced MLA from rat brain homogenates with a Ki of 27 nM.[33]

side chains. X-ray crystal structures of the extracellular domain of an α1 subunit from muscle nAChR (bound to α-bungarotoxin),[11] and prokaryotic orthologs[12−14] have provided further key insights to nAChR structure. A high-resolution

crystallographic structure of a soluble homopentameric nAChR homologue, the acetylcholine binding protein (AChBP) isolated from the freshwater snail *Lymnaea stagnalis*, was reported by the Sixma group in 2001.[15] Since that time, X-ray crystallographic data from various AChBP and nAChR agonist or antagonist complexes have been solved at high resolution to provide a rather precise picture of how nicotinic ligands interact with homologous proteins in the binding site.[16−18] Moreover, various AChBPs exhibit properties and ligand affinities similar to those of nAChRs, suggesting structural similarities.[19,20]

It is of note, while AChBPs have 20−26% overall sequence identity to nAChR extracellular domains, sequence homology within the orthosteric ligand-binding domain is much higher. Further, two recent reports have examined mutations of AChBPs with the aim of producing $\alpha7$ recognition domains with even higher similarity. Crystal structures have been obtained for apo and epibatidine bound $\alpha7$-nAChR chimeras,[21] with three additional Ac-AChBP mutants showing further structural features both in the apo form and with a variety of nicotinic ligands.[22] These may provide realistic templates for structure-aided drug design.

The $\alpha7$ nAChR is one of the most abundant subtypes in the human central nervous system[23] as well as one of the most extensively studied nAChRs. This subtype is distinguished by its high permeability to calcium and its rapid activation and desensitization kinetics.[24] Because of its prevalence in brain regions such as the hippocampus and cerebral cortex, the $\alpha7$ nAChR is strongly implicated in cognition, i.e., memory and learning processes. Design of subtype selective ligands is a predominant objective of current nAChR drug development efforts. Therefore, a full understanding of the binding behavior of ligands to the $\alpha7$ nAChR is an important step toward the rational design of potential subtype-directed therapeutics.

In this investigation, homology models of the extracellular domain of the human $\alpha7$ nAChR subtype were derived based on high-resolution crystal structures of AChBP. A variety of nicotinic ligands were then docked into the $\alpha7$ binding site. On the basis of analyses of the observed ligand poses within the ligand binding domain, we propose that $\alpha7$ ligands from different chemotypes may bind to this receptor in a variety of ways and that key ligand−protein residue interactions are utilized in each region to drive binding affinity. These studies should have utility in aiding the design of future $\alpha7$ ligands.

■ COMPUTATIONAL METHODS

nAChR Orthosteric Ligand Collection and Preparation. The past decade has seen an enormous amount of effort expended on the design and discovery of ligands targeting nAChRs, especially for $\alpha4\beta2$ and $\alpha7$, which are two predominantly expressed subtypes in the mammalian brain. Representative orthosteric ligands representing various chemotypes, both from literature and our internal compound database, were selected for docking studies. Structures along with their $\alpha4\beta2$ and $\alpha7$ nAChR binding affinity K_i values are shown in Table 1. Structures of these nAChR orthosteric ligands were constructed using MOE (version 2010.10, Chemical Computing Group, Montreal, Canada). The protonation states of ligands were assigned using the Wash module at pH 7.4 in MOE. Conformational searching was used to identify local minima and a final three-dimensional conformation was energy-minimized with the molecular mechanics MMFF94x force field in MOE, as an initial starting point for docking experiments.

Homology Modeling of the Ligand Binding Domain (LBD) of Human $\alpha7$ nAChR. Models of the extracellular domain of the human $(\alpha7)_5$ protein were constructed from the X-ray structure of the epibatidine-bound form of *Aplysia* AChBP (PDB entry: 2BYQ[39] at 3.4 Å resolution), using the MODELER module[40] in the Discovery Studio (DS version 3.1) (Accelrys, Inc.) software package. Sequence alignment was performed using the Align Multiple Sequence protocol in DS using a progressive pairwise alignment algorithm and the alignment scoring matrix was set to be BLOSUM. The final alignment was adjusted manually based on the sequence alignment by Celie et al.[41] using the sequence edit panel. Each subunit of the homopentameric $\alpha7$ structure was built using the corresponding subunit in the AChBP template, and all five subunits were created simultaneously. Disulfide bridge restraints were added and loops were refined. The five epibatidine ligands, taken from the cocrystal structure, were copied and duplicated in the new $\alpha7$ homology model. The initial pentameric model was further refined by carefully performing a series of energy minimizations using Macro-Model[42] (Maestro, Schrodinger, Inc.). The architecture and stereochemical quality of the derived protein structures were assessed by the software Procheck.[43] The overall quality of the final model structure was determined by ERRAT.[44]

Ligand Docking. Docking studies were carried out using CDOCKER,[45,46] a CHARMm-based[47] molecular dynamics simulated-annealing program that treats the ligand as fully flexible while maintaining a rigid receptor. Standard protonation state at physiological pH was used for all ligands, i.e., with protonation on each quinuclidine nitrogen and the conformational analysis of each protonated ligand was carried out using MOE package with low mode setting. For every docking experiment, diverse random conformations per ligand were generated and docked into a binding domain defined as a sphere (12 Å radius) around the location of the epibatidine ligand used during refinement of the model with default options. Ten different poses were generated for each protonated ligand. Final poses were ranked based on the CDOCKER energy combined with geometric matching quality.

■ RESULTS AND DISCUSSION

Sequence Alignment and Homology Modeling. Sequence alignment provides a measure of homology between the amino-terminal extracellular domain of the $\alpha7$ nAChR subtype and AChBP and shows 25.9% sequence identity and 43.0% sequence similarity. The derived homology model of the ligand binding domain (LBD) for the $\alpha7$ nAChR was composed of an N-terminal α-helix along with seven strands. Our final, refined structure showed an overall quality factor of 71% by ERRAT with 86% of residues in the most-favored region of the Ramachandran plot (Procheck). As expected, given the low number of insertions and deletions, the model did not exhibit major structural differences from the template. This homopentameric $(\alpha7)_5$ model shows 5-fold symmetry, with LBDs formed from each pair of $\alpha7$ subunits, i.e. a principal face (α) and a complementary face (β). Of note is the high aromatic character of the LBD, i.e. the typical aromatic cage at the binding pocket[17] (see Figure 1), formed by two tryptophan residues from the principal side and the complementary side labeled αTrp147 and βTrp53, respectively, along with three tyrosine residues, i.e. αTyr91, αTyr186, and αTyr193. Further, in the occupied form of the LBD, there is close proximity between the disulfide bond (αCys188 and αCys189) from the
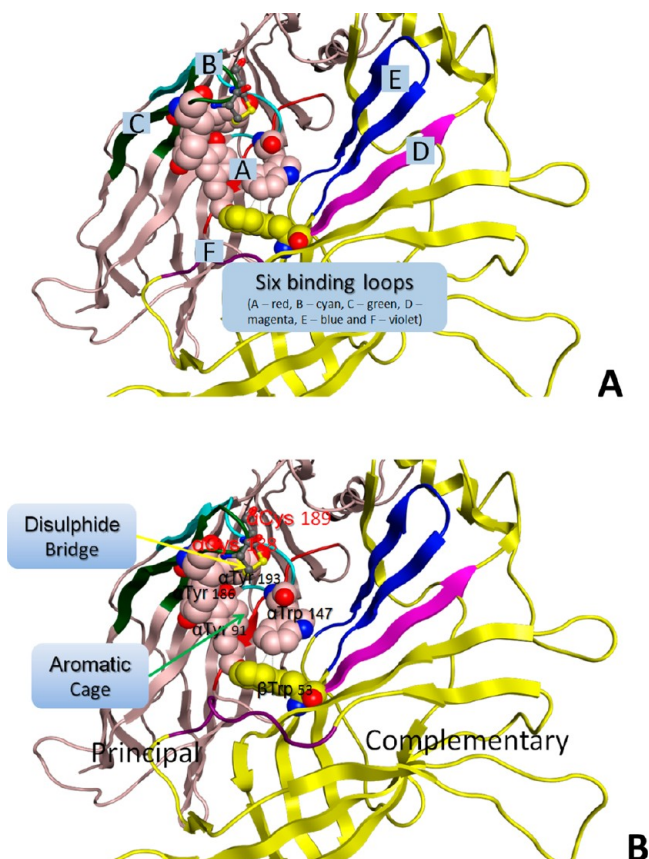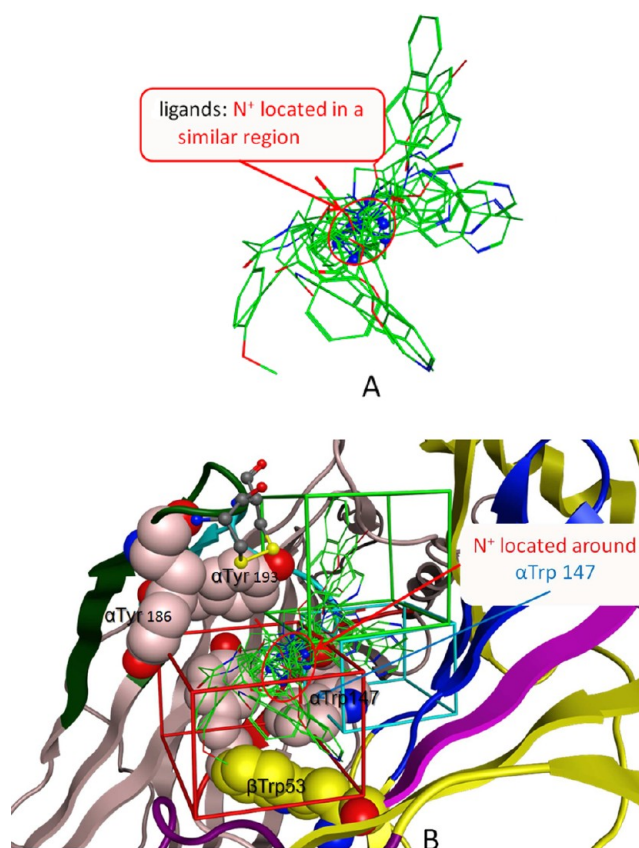
Figure 1. Two adjacent subunits [(principal) light pink and (complementary) yellow] showing: (**A**) positions of the six binding loops [(A) red, (B) cyan, (C) green, (D) magenta, (E) blue, and (F) violet], (**B**) aromatic cage (αTrp147, βTrp53 and αTyr91, αTyr186 and αTyr193 space filling) and the disulfide bridge (αCys188 and αCys189 stick).

Figure 2. (**A**) Superimposed binding poses of various ligands, illustrating exploration of three different regions within the ligand binding domain. (**B**) Binding poses found within the ligand-binding domain of the human α7 nAChR, subdivided into three regions: (1) cyan, (2) green, and (3) red.

C-loop and the key αTrp147. A feature found in most AChBP-nicotinic ligand cocrystal structures.

Docking. In the past decade, a number of studies have examined molecular docking of nicotinic ligands to various nAChRs or AChBPs[48−52] in attempts to provide increased insight into those features of importance for high affinity and provide guidance in the design of potential nAChR therapeutics. However, most of these ligand binding studies have focused only on a homogeneous series or on a small set of nicotinc ligands. In that same period of time, significant effort on the design and synthesis of nicotinic ligands has led to substantial diversity in nAChR ligand chemotypes. We have chosen a diverse set of nicotinic ligands with a wide range of α7 binding affinities from the literature as well as our own in-house collection, as a set of ligands to perform docking studies using our α7 nAChR model. This set was designed to probe various potential interactions within the LBD and to provide some insight into those interactions that lead to high affinity and/or selectivity.

For each nicotinic ligand, highly ranked poses were selected using the criteria described above. In all cases, docked poses show positively charged nitrogen atoms (cationic centers of α7 nAChR ligands) within a relatively small region of the LBD and near the conserved αTrp147 residue. In these docking studies, it is likely that these orientations are at least in part driven by a hydrogen bond between the protonated cationic center hydrogen(s) and the backbone carbonyl of αTrp147 (observed
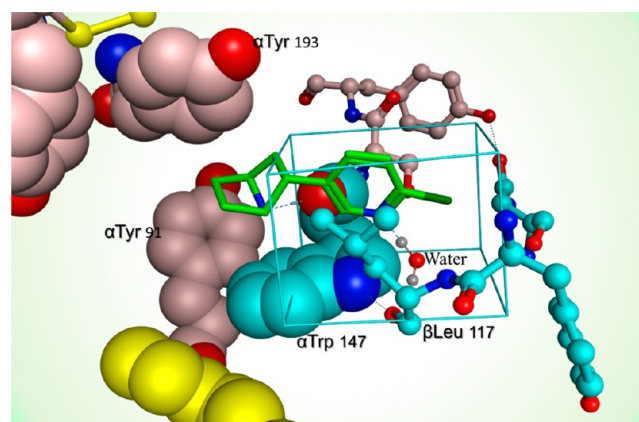
Figure 3. Highest ranked docked pose of epibatidine in the α7 nAChR model, showing cationic center to tyrptophan carbonyl hydrogen bond and water mediated hydrogen bond to the pyridinyl nitrogen.

experimentally in various AChBP-nicotinic ligand cocrystal structures[17,18]). It has been proposed that further contributions to affinity in actual ligand−protein interactions comes from a strong cation-π interaction between the cationic center and this same conserved tryptophan, as well as potentially other aromatic residues in the highly aromatic LBD (for example αTyr91 and αTyr193) and that this cation-π interaction plays an essential role in both nAChR function and binding.[53−55] These cation-π interactions may not be fully accounted for in
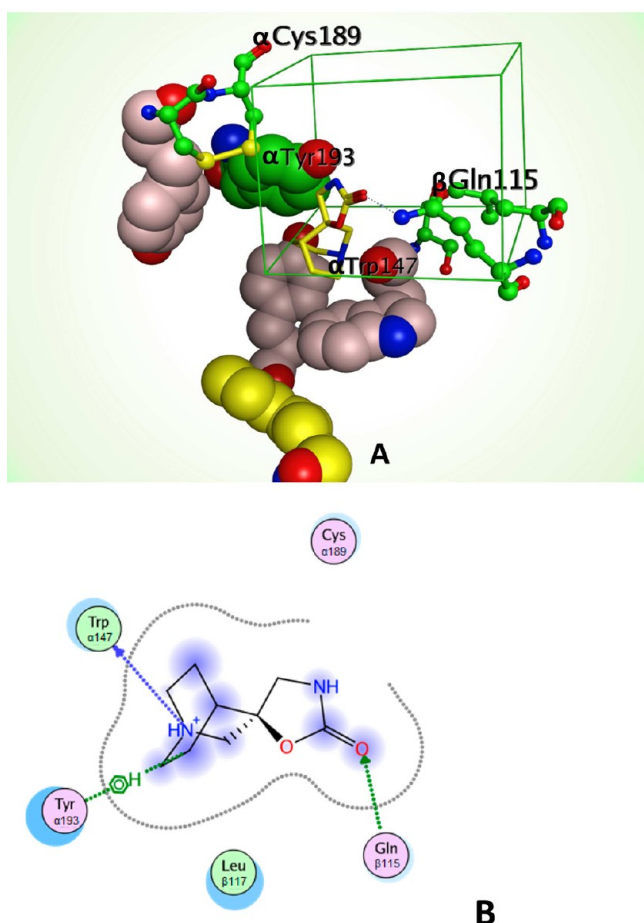
Figure 4. (A) Docked pose of AR-R1779. (B) 2D representation of interactions between AR-R1779 and α7 nAChR. Hydrogen bond interactions: (blue arrow) backbone acceptor; (green arrow) side chain donor.
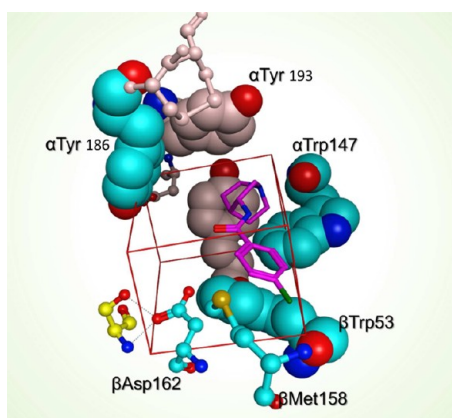
Figure 5. Top-ranked pose of PNU-282987 within the α7 nAChR model (Region 3).

the docking algorithm or scoring function and could lead to somewhat different poses than those found in actual cocrystal structures.

A second pharmacophoric element required for nicotinic ligands is a hydrogen bond acceptor, generally located within 4.5−7.5 Å of the cationic center.[56] In this study, docked poses of various ligands show hydrogen bond formation within the binding domain, however binding sites and/or orientation of

hydrogen bonds can vary considerably for structurally diverse ligands. Analysis of all nicotinic ligand poses docked within the LBD (Figure 2) shows that these various hydrogen bond acceptor groups adjacent to the cationic center may occupy at least three different areas within the binding domain. For clarity, we subdivide the LBD into three regions (1, 2, and 3) and explore their possible role for nAChR subtype affinity and selectivity.

Region 1 is located in the area near αTrp147 (principal face) and extends to βAsn105 as well as βLeu117 from Loop-E of the complementary face. This region is a common binding area for nicotinic ligands and encompasses positions of the pyridinyl group for nicotine, epibatidine, and varenicline cocrystallized with AChBP, where each pyridine group shares a similar set of interactions and orientations. Ligands with multiple subtype nAChR affinities, such as epibatidine and varenicline, show highly ranked poses in this region. Illustrated in Figure 3 is the top-ranked docked pose of epibatidine in the α7 nAChR model, showing the expected cation-π and hydrogen bond interactions with αTrp147, as well as a water molecule mediated hydrogen bond interaction between the pyridinyl nitrogen and βLeu117 amide backbone. This docked pose has a similar orientation and interactions in the α7 nAChR model as those found for epibatidine in Ac-AChBP[18] and a recently published X-ray crystal structure with a α7-AChBP chimera.[21] Additionally, this docked pose shows that the carbon adjacent to N^+, which carries a large partial positive charge, is close to αTyr193 and αTyr91 within the aromatic cage of α7 nAChR binding domain and may contribute to further cation-π interactions. Such interactions have recently been described by Dougherty's group to play a critical role in α7 nAChR binding.[55]
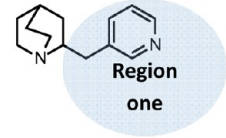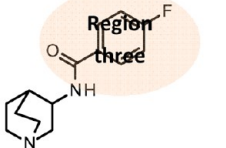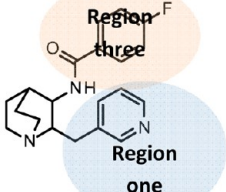
Additional potential interactions are illustrated by the docked pose of the spiro quinuclidinyl derivative AR-R1779 (Figure 4), which displays a direct hydrogen bond interaction with residue βGln115 of the α7 nAChR model (a similar docked pose has been cited previously by Huang).[48] This interaction with the hydrophilic residue βGln115 may be unique for the α7 subtype since nearly all other nAChRs present hydrophobic residues in this area of region 2. Ligands interacting with region 2 probe an area spanning from Loop-C to Loops-B and -E and may contribute to α7-selectivity over other nAChR subtypes.

The top ranked pose of the quinuclidine derivative PNU-282987 probes an area surrounded by several additional aromatic residues, defined as region 3 (Figure 5). Ligands interacting with region 3 probe the area including Loop-D and the two very flexible Loops-C and -F. PNU-282987 is a high affinity α7 ligand and we propose that region 3 contributes to α7-selectivity over other nAChR subtypes. However, serotonin 5-HT3 ligands also appear to bind to this region based on an AChBP cocrystal structure with the 5-HT3 receptor antagonist tropisetron.[57]

These examples show that ligands with a central cationic core but with groups interacting at one or more of the regions within the ligand-binding domain demonstrate differing tendencies for both binding affinity and selectivity. Compounds that probe only region 1 tend to be nonselective and bind with high affinity at both α4β2 and α7, for example epibatidine and varenicline; ligands such as AR-R17779, that probe primarily region 2, show moderate α7 nAChR affinity; ligands that interact primarily with region 3 tend to have high α7 nAChR and further, have the potential for 5HT-3 affinity. This latter case is illustrated by PUN-282987 (rat α7 nAChR K_i = 26 nM and 5HT-3 K_i = 930 nM[58]).

Table 2. Comparison of Human α7 and α4β2 nAChR Affinities between Single Region Interaction and Multiple Region Interaction Ligands

Structure	Reference	Human α7 Ki (nM)[a]	Human α4β2 Ki (nM)[b]
Region one	59	240	9.5
Region three	33	880	>5000
Region three / Region one	4	31	650
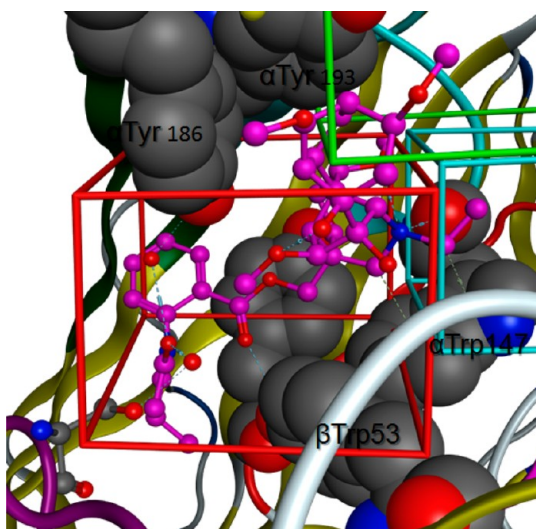
Figure 6. MLA (violet) in the complex of MLA and AChBP and the relative position of three region boxes.

Figure 7. 2D diagram of interactions between TC-7020 and human α7 nAChR generated by the MOE software package.

Table 2 demonstrates that a combination of multiple region interactions both enhances α7 nAChR binding affinity as well as selectivity. For instance, docked poses of the pyridinyl methyl quinuclidine (top row of Table 2) show interactions primarily with region 1. This compound exhibits more than 20-fold greater affinity for human α4β2 compared to human α7 nAChR subtypes. Conversely, the quinuclidine with a 3-position amide shown in the middle row of Table 2 has interactions primarily within region 3 and has moderate human

α7 nAChR affinity but very little binding affinity at α4β2. Combining both of these moieties with the quinuclidine nucleus gives the third compound in Table 2. Docked poses for this compound show interactions both in region 1 and region 3. This compound achieves high affinity at human α7 nAChR and exhibits more than 20-fold selectivity over human α4β2 nAChR. It is of further note that the cocrystal structure of AChBP with the selective α7 antagonist methyllycaconitine (MLA)[18] shows interactions in all 3 regions, i.e., MLA has strong hydrogen bond and cation-π interactions in region 1, as well as π−π and hydrogen bond interactions in regions 2 and 3 (Figure 6). During lead-optimization studies, we have achieved even more selective α7 nAChR subtype ligands[61] by
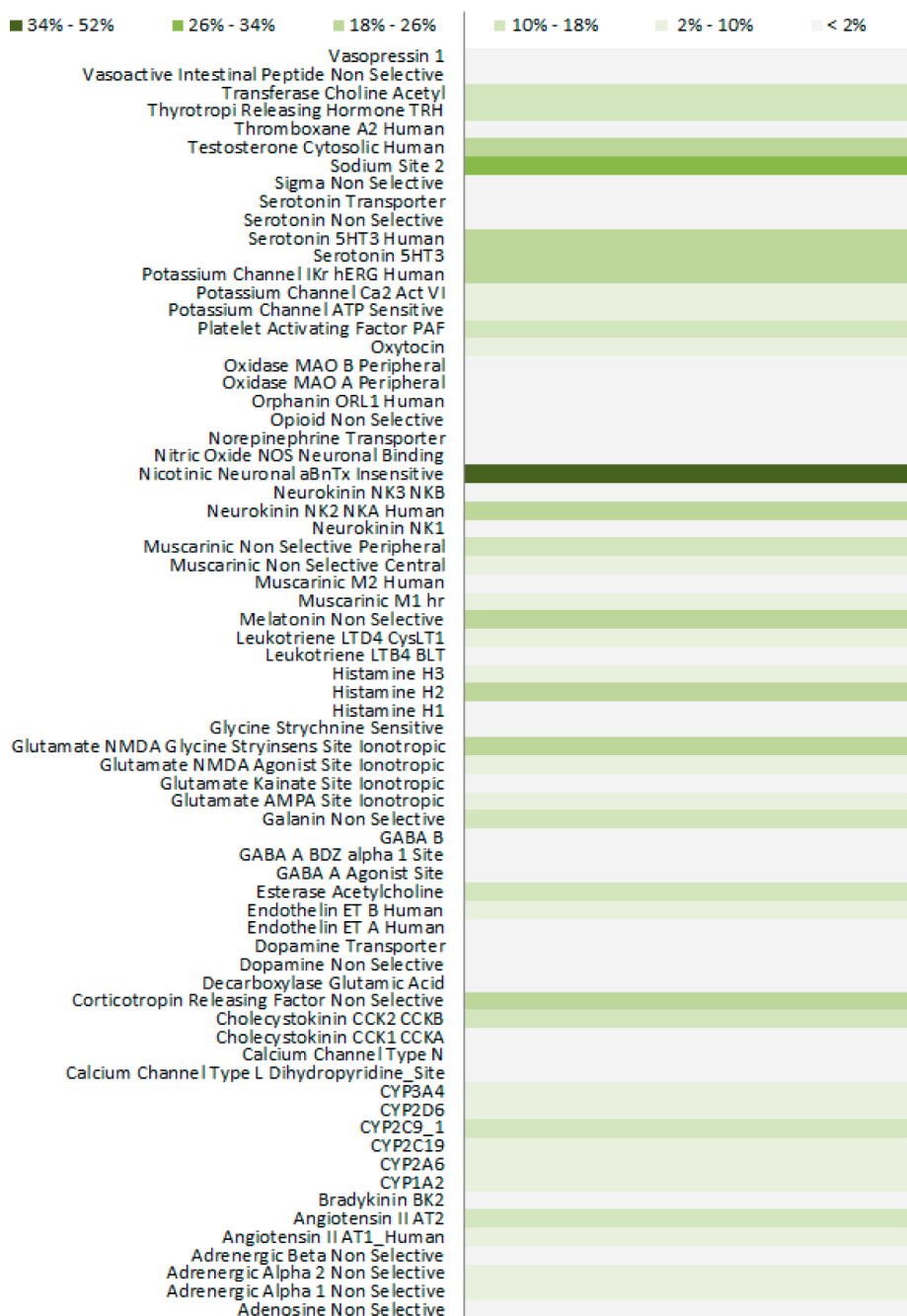
Figure 8. Biological profile of TC-7020. Shown is a heat map expressing percent inhibition values at 10 μM for TC-7020 in 71 bioassays. In the coloring scheme used for this heat map, percent inhibition values of 2%, 10%, 18%, 26%, and 52% are expressed by a gradient varying from white to light green through dark green, respectively.

manipulating substitution of those moieties that interact with region three.

In an attempt to better understand the influence of the 2-(arylmethyl) moiety in 2-(pyridin-3-ylmethyl) quinuclidine amides, we have docked TC-7020 and its analogs to the human α7 nAChR model. As expected, the 2D diagram of ligand−receptor interactions (Figure 7) shows that TC-07020 sits between two adjacent subunits with the protonated quinuclidine nitrogen lying at the center of the "aromatic cluster"[60] that forms the LBD. Proximity of the cationic center of the ligand with these LBD aromatic residues illustrates the potential for not only a strong cation-π interaction with αTrp147 but the potential for similar interactions with αTyr91

and αTyr93. The quinuclidine 3-position amide of TC-7020 probes from Loop-E to Loops-D and -F, i.e. region 3, with the thiophene proximal to βTrp53 allowing for a potential π−π interaction in that region. Similar binding poses have been observed in the published cocrystal structures of *Aplysia* AChBP receptor in complex with the α7 nAChR ligands 3-(2,4-dimethoxybenzylidene) anabaseine and its 4-hydroxy metabolite.[18] Docked poses of the 2-(pyridinylmethyl) moiety occupy region 1 and show potential water mediated hydrogen bond interactions similar to those found in many of the pyridine-containing nicotinic ligand cocrystal structures with various AChBPs. These multiple, key interactions enhance binding

affinity and produce compounds with some of the highest $\alpha 7$ binding affinities known.[61]

Besides increased nAChR affinity and selectivity, an additional benefit obtained by introduction of interactions with regions 1 and 3 is illustrated by the lack of off-target binding for TC-7020. Figure 8 shows a heat map for TC-7020 screened against more than 70 non-nAChR and nAChR target receptors. The only displacement that showed significant signal was that for the bungarotoxin insensitive nAChR assay (50.8% inhibition at 10 μm), indicating that TC-7020 was clean against 70 other off-target receptors. Further, TC-7020 was examined for its effect on the maximum amplitude of tail currents determined from traces obtained on voltage-clamped cells recombinantly expressing the human ether-a-go-go gene (hERG). Inhibition at 3, 10, 30, and 100 μM concentrations indicated that the IC_{50} was greater than 100 μM. These results for TC-7020 (and other compounds) demonstrate that optimization of interactions with both region one and three lead to compounds that achieve selectivity and high affinity at $\alpha 7$ compared to other nAChR subtypes and compounds that show little off-target activity.

CONCLUSION

The $\alpha 7$ nAChR is an important target based on association with a number of human disorders in which sensory gating plays a role. Docking results on a chemotypically diverse ligand set with a homology model of the $\alpha 7$ nAChR show different interactions within the ligand binding site. These interactions may be subclassified into three distinct regions, where each region plays a role in general nAChR binding or in the case of regions 2 and 3, appear to be associated with either increased affinity or selectivity at $\alpha 7$, or both. Docking studies indicate that $\alpha 7$ binding affinity for ligands containing various chemotypes are enhanced by interactions with key residues in these different regions. In particular, these computational studies have shown that our novel series of 2-(pyridin-3-ylmethyl) quinuclidine 3-position amides interact with the central cationic interaction site near αTrp147, as well as with region 1 and Loop-F in region 3 of the $\alpha 7$ nAChR, with these latter interactions driven by hydrogen bonding, steric, and $\pi-\pi$ interactions. In total, the result is enhanced binding affinity at the $\alpha 7$ nAChR subtype and increased selectivity over other nAChRs, with an additional benefit of reduced off-target interactions. Homology models of this type coupled with docking studies and region analysis can serve as a tool for the rational design of new, selective nAChR ligands.

AUTHOR INFORMATION

Corresponding Author
*Current mailing address: Cubist Pharmaceuticals, 65 Hayden Avenue, Lexington MA 02421. E-mail: yunde.xiao@cubist.com.

Notes
The authors declare no competing financial interest.

REFERENCES

(1) Changeux, J. P.; Bertrand, D.; Corriger, P. J.; Dehaene, S.; Edelstein, S.; Lena, C.; Le Novere, N.; Marubio, L.; Picciotto, M.; Zoli, M. Brain Nicotinic Receptors: Structure and Regulation, Role in leaning and Reinforcement. *Brain Res. Rev.* **1998**, *26*, 198−216.

(2) Karlin, A. Emerging Structure of the Nicotinic Acetylcholine Receptors. *Nat. Rev. Neurosci.* **2002**, *3*, 102−114.

(3) Cederholm, J. M.; Schofield, P. R.; Lewis, T. M. Gating Mechanisms in Cys-loop Receptors. *Eur. Biophys. J.* **2009**, *39*, 37−49.

(4) Romanelli, M. N.; Gratteri, P.; Guandalini, L.; Martini, E.; Bonaccini, C.; Gualtieri, F. Central Nicotinic Receptors: Structure, Function, Ligands, and Therapeutic Potential. *ChemMedChem* **2007**, *2*, 746−767.

(5) Mudo, G.; Belluardo, N.; Fuxe, K. Nicotinic Receptor Agonists as Neuroprotective/Neurotrophic Drugs. Progress in Molecular Mechanisms. *J. Neural Transm.* **2007**, *114*, 135−147.

(6) Keating, G. M.; Siddiqui, M. A. Varenicline: a Review of its Use as an Aid to Smoking Cessation Therapy. *CNS Drugs.* **2006**, *20*, 945−960.

(7) Paterson, D.; Nordberg, A. Neuronal Nicotinic Receptors in the Human Brain. *Prog. Neurobiol.* **2000**, *61*, 75−111.

(8) Mazzaferro, S.; Benallegue, N.; Carbone, A.; Gasparr, F.; Vijayan, R.; Biggin, P. C.; Moroni, M.; Bermudez, I. Additional Acetylcholine Binding Site at $\alpha 4/\beta 4$ Interface of $(\alpha 4\beta 2)2\alpha 4$ Nicotinic Receptor Influences Agonist Sensitivity. *J. Biol. Chem.* **2011**, *286*, 31043−31054.

(9) Albuquerque, E. X.; Pereira, E. F. R.; M Alkondon, M.; Rogers, S. W. Mammalian Nicotinic Acetylcholine Receptors: From Structure to Function. *Physiol. Rev.* **2009**, *89*, 73−120.

(10) Unwin, N. Refined Structure of the Nicotinic Acetylcholine Receptor at 4Å. *J. Mol. Biol.* **2005**, *346*, 967−989.

(11) Dellisanti, C. D.; Yao, Y.; Stroud, J. C.; Wang, Z. Z.; Chen, L. Crystal Structure of the Extracellular Domain of nAChR $\alpha 1$ Bound to Alpha-Bungarotoxin at 1.94 Å Resolution. *Nat. Neurosci.* **2007**, *10*, 953−962.

(12) Hilf, R. J.; Dutzler, R. X-Ray Structure of a Prokaryotic Pentameric Ligand-Gated ion Channel. *Nature* **2008**, *452*, 375−379.

(13) Hilf, R. J.; Dutzler, R. Structure of a Potentially Open State of a Proton-Activated Pentameric Ligand-Gated Ion Channel. *Nature* **2009**, *457*, 115−118.

(14) Bocquet, N.; Nury, H.; Baaden, M.; Poupon, C. L.; Changeux, J.-P.; Delarue, M.; Corringer, P.-J. X-Ray Structure of a Pentameric Ligand-Gated Ion Channel in an Apparently Open Conformation. *Nature* **2009**, *457*, 111−114.

(15) Brejc, K.; van Dijk, W. J.; Klaassen, R. V.; Schuurmans, M.; van Der Oost, J.; Smit, A. B.; Sixma, T. K. Crystal Structure of an Ach-Binding Protein Reveals the Lignd-Binding Domain of Nicotinic Receptors. *Nature* **2001**, *411*, 261−268.

(16) Celie, P. H.; van Rossum-Fikkert, S. E.; van Dijk, W. J.; Brejc, K.; Smit, A. B.; Sixma, T. K. Nicotine and Carbamylcholine Binding to Nicotinic Acetylcholine Receptors as Studied in AChBP Crystal Structures. *Neuron* **2004**, *41*, 907−914.

(17) Hansen, S. B.; Talley, T. T.; Radic, Z.; Taylor, P. Structural and Ligand Recognition Characteristics of an Acetylcholine-Binding Protein from *Aplysia Californica*. *J. Biol. Chem.* **2004**, *279*, 24197−24202.

(18) Hibbs, R. E.; Sulzenbacher, G.; Shi, J.; Talley, T. T.; Conrod, S.; Kem, W. R.; Taylor, P.; Marchot, P.; Bourne, Y. Structural Determinants for Interaction of Partial Agonists with Acetylcholine Binding Protein and Neuronal Alpha7 Nicotinic Acetylcholine Receptor. *EMBO J.* **2009**, *28*, 3040−3051.

(19) Hansen, S. B.; Radic, Z.; Talley, T. T.; Molles, B. E.; Deerinck, T.; Tsigelny, I.; Taylor, P. Tryptophan Fluorescence Reveals Conformational Changes in the Acetylcholine Binding Protein. *J. Biol. Chem.* **2002**, *277*, 41299−41302.

(20) Hansen, S. B.; Radic, Z.; Talley, T. T.; Radic, Z.; Taylor, P. Ligand Binding Characteristics of the Acetylcholine Binding Proteins from *Lymnaea stagnalis* and *Aplysia Californica*. *Faseb J.* **2003**, *17*, A641−A641.

(21) Li, S.-X.; Huang, S.; Bren, N.; Noridomi, K.; Dellisanti, C. D.; Sine, S. M.; Chen, L. Ligand-Binding Domain of an $\alpha 7$-Nicotinic Receptor Chimera and its Complex with Agonist. *Nat. Neurosci.* **2011**, *14*, 1253−1259.

(22) Akos, N.; Palmer, T. Recognition Domain from the Acetylcholine-binding Protein: Crystallographic and Ligand Selectivity Analyses. *J. Biol. Chem.* **2011**, *286*, 42555−42565.

(23) Bencherif, M. Neuronal Nicotinic Receptors as Novel Targets for Inflammation and Neuroprotection: Mechanistic Considerations and Clinical Relevance. *Acta Pharmacol. Sin.* **2009**, *30*, 702−714.

(24) Dajas-Bailador, F.; Wonnacott, S. Nicotinic Acetylcholine Receptors and the Regulation of Neuronal Signaling. *Trends Pharmacol. Sci.* **2004**, *25*, 317–324.

(25) Fiebre, C. M.; Meyer, E. M.; Henry, J. C.; Muraskin, S. I.; Kem, W. R.; Papke, R. L. Characterization of a Series of Anabaseine-Derived Compounds Reveals that the 3-(4)-Dimethylaminocinnamylidine Derivative is a Selective Agonist at Neuronal Nicotinic α7/^{125}I-α-Bungarotoxin Receptor Subtypes. *Mol. Pharmacol.* **1995**, *47*, 164–171.

(26) Mullen, G.; Napier, J.; Balestra, M.; DeCory, T.; Hale, G.; Macor, J.; Mack, R.; Loch, J., III; Wu, E.; Kover, A.; Verhoest, P.; Sampognaro, A.; Phillips, E.; Zhu, Y.; Murray, R.; Griffith, R.; Blosser, J.; Gurley, D.; Machulskis, A.; Zongrone, J.; Rosen, A.; Gordon, J. (-)-Spiro[1-Azabicyclo[2.2.2]Octane-3,5′-Oxazolidin-2′-one], a Conformationally Restricted Analogue of Acetylcholine, is a Highly Selective Full Agonist at the α7 Nicotinic Acethylcholine Receptor. *J. Med. Chem.* **2000**, *43*, 4045–4050.

(27) Fletcher, S. R.; Baker, R.; Chambers, M. S.; Hobbs, S. C.; Mitchell, P. J. Total Synthesis and Determination of the Absolute Configuration of Epibatidine. *J. Org. Chem.* **1994**, *59*, 1771–1778.

(28) Mazurov, A.; Miao, L.; Klucik, J. *Heteroaryl-Substituted Diazabicycloalkanes, Methods for its Preparation and Use Thereof.* US Pat. 7732607, 2010.

(29) Azuma, R.; Komuro, M.; Korsch, B. H.; Andre, J. C.; Onnagawa, O.; Black, S. R.; Mathews, J. M. Metabolism and Disposition of GTS-21, a Novel Drug for Alzheimer's Disease. *Xenobiotica* **1999**, *29*, 747–762.

(30) Kombo, D. C.; Mazurov, A. A.; Chewning, J.; Hammond, P. S.; Tallapragada, K.; Hauser, T. A.; Speake, J.; Yohannes, D.; Caldwell, W. S. Discovery of Novel α7 Nicotinic Acetylcholine Receptor Ligands via Pharmacophoric and Docking Studies of Benzylidene Anabaseine Analogs. *Bioorg. Med. Chem. Lett.* **2012**, *22*, 1179–1186.

(31) Coe, J. W.; Brooks, P. R.; Vetelino, M. G.; Wirtz, M. C.; Arnold, E. P.; Huang, J.; Sands, S. B.; Davis, T. I.; Lebel, L. A.; Fox, C. B.; Shrikhande, A.; Heym, J. H.; Schaeffer, E.; Rollema, H.; Lu, Y.; Mansbach, R. S.; Chambers, L. K.; Rovetti, C. C.; Schulz, D. W.; Tingley, F. D.; O'Neill, B. T. Varenicline: an α4β2 Nicotinic Receptor Partial Agonist for Smoking Cessation. *J. Med. Chem.* **2005**, *48*, 3474–3477.

(32) Biton, B.; Bergis, O.; Galli, F.; Nedelec, A.; Lochead, A.; Jegham, S.; Godet, D.; Lanneau, C.; Santamaria, R.; Chesney, F.; Leonardon, J.; Granger, P.; Debono, M. W.; Bohme, G. A.; Sgard, F.; Besnard, F.; Graham, D.; Coste, A.; Oblin, A.; Curet, O.; Vige, X.; Voltz, C.; Rouquie, L.; Souilhac, J.; Santucci, V.; Gueudet, C.; Francon, D.; Steinberg, R.; Griebel, G.; Oury-Donat, F.; George, P.; Avenet, P.; Scatton, B. SSR180711, a Novel Selective α7 Nicotinic Receptor Partial Agonist: (1) Binding and Functional Profile. *Neuropsychopharmacology* **2007**, *32*, 1–16.

(33) Bodnar, A. L.; Cortes-Burgos, L. A.; Cook, K. K.; Dinh, D. M.; Groppi, V. E.; Hajos, M.; Higdon, N. R.; Hoffmann, W. E.; Hurst, R. S.; Myers, J. K.; Rogers, B. N.; Wall, T. M.; Wolfe, M. L.; Wong, E. Discovery and Structure-Activity Relationship of Quinuclidine Benzamides as Agonists of α7 Nicotinic Acetylcholine Receptors. *J. Med. Chem.* **2005**, *48*, 905–908.

(34) Marrero, M. B.; Lucas, R.; Salet, C.; Hauser, T. A.; Mazurov, A.; Lippiello, P. M.; Bencherif, M. An α7 Nicotinic Acetylcholine Receptor-Selective Agonist Reduces Weight Gain and Metabolic Changes in a Mouse Model of Diabetes. *J. Pharmacol. Exp. Ther.* **2010**, *332*, 173–180.

(35) Phillips, E.; Mack, R.; Macor, J.; Semus, S. *Spiroazabicyclic Heterocyclic Compounds.* US Pat. 6706878, 2004.

(36) Haydar, S. N.; Ghiron, C.; Bettinetti, L.; Bothmann, H.; Comery, T. A.; Dunlop, J.; La Rosa, S.; Micco, I.; Pollastrini, M.; Quinn, J.; Roncarati, R.; Scali, C.; Valacchi, M.; Varrone, M.; Zanaletti, R. SAR and Biological Evaluation of SEN12333/WAY-317538: Novel Alpha 7 Nicotinic Acetylcholine Receptor Agonist. *Bioorg. Med. Chem.* **2009**, *17*, 5247–5258.

(37) Davies, A. R.; Hardick, D. J.; Blagbrough, I. S.; Potter, B. V.; Wolstenholme, A. J.; Wonnacott, S. Characterization of the Binding of [^{3}H]methyllycaconitine: a New Radioligand for Labeling α7- Type

(38) Lippiello, P. M.; Fernades, K. G. The Binding of L-[^{3}H] Nicotine to a Single Class of High Affinity Sites in Rat Brain Membranes. *Mol. Pharmacol.* **1986**, *29*, 448–454.

(39) Celie, P. H.; Kasheverov, I. E.; Mordvintsev, D. Y.; Hogg, R. C.; van Nierop, P.; van Elk, R.; van Rossum-Fikkert, S. E.; Zhmak, M. N.; Bertrand, D.; Tsetlin, V.; Sixma, T. K.; Smit, A. B. Crystal Structure of Nicotinic Acetylcholine Receptor Homolog AChBP in Complex with an Alpha-Conotoxin PnIA Variant. *Nat. Struct. Mol. Biol.* **2005**, *12*, 582–588.

(40) Sali, A.; Blundell, T. L. Comparative Protein Modeling by Satisfaction of Spatial Restraints. *J. Mol. Biol.* **1993**, *234*, 779–815.

(41) Celie, P. H. N.; Klaassen, R. V.; van Rossum-Fikkert, S. E.; van Elk, R.; van Nierop, P.; Smit, A. B.; Sixma, T. K. Crystal Structure of Acetylcholine-binding Protein from *Bulinus truncatus* Reveals the Conserved Structural Scaffold and Sites of Variation in Nicotinic Acetylcholine Receptors. *J. Biol. Chem.* **2005**, *280*, 26457–26466.

(42) Mohamadi, F.; Richards, N. G. J.; Guida, W. C.; Liskamp, R.; Lipton, M.; Caufield, C.; Chang, G.; Hendrickson, T.; Still, W. C. MacroModel: an Integrated Software System for Modeling Organic and Bioorganic Molecules Using Molecular Mechanics. *J. Comput. Chem.* **1990**, *11*, 440–467.

(43) Laskowski, R. A.; MacArthur, M. W.; Moss, D. S.; Thornton, J. M. PROCHECK: a Program to Check the Stereochemical Quality of Protein Structure. *J. Appl. Crystallogr.* **1993**, *26*, 283–291.

(44) Colovos, C.; Yeates, T. O. Verification of Protein Structures: Patterns of Nonbonded Atomic Interactions. *Protein Sci.* **1993**, *2*, 1511–1519.

(45) Wu, G.; Robertson, D. H.; Brooks, C. L.; Vieth, M. Detailed Analysis of Grid-based Molecular Docking: a Case Study of CDOCKER − a CHARMm-based MD Docking Algorithm. *J. Med. Chem.* **2003**, *24*, 1549–1562.

(46) Erickson, J. A.; Jalaie, M.; Robertson, D. H.; Lewis, R. A.; Vieth, M. Lessons in Molecular Recognition: the Effects of Ligand and Protein Flexibility on Molecular Docking Accuracy. *J. Med. Chem.* **2004**, *47*, 45–55.

(47) Brooks, B. R.; Bruccoleri, R. E.; Olafson, B. D.; States, D. J.; Swaminathan, S.; Karplus, M. CHARMm: a Program for Macromolecular Energy, Minimization, and Dynamics Calculations. *J. Comput. Chem.* **1983**, *4*, 187–217.

(48) Huang, X.; Zheng, F.; Chen, X.; Crooks, P. A.; Dwoskin, L. P.; Zhan, C. G. Modeling Subtype-Selective Agonists Binding with α4β2 and α7 Nicotinic Acetylcholine Receptors: Effects of Local Binding and Long-Range Electrostatic Interactions. *J. Med. Chem.* **2006**, *49*, 7661–7674.

(49) Huang, X.; Zheng, F.; Stokes, C.; Papke, R. L.; Zhan, C. G. Modeling Binding Modes of Alph7 Nicotinic Acetylcholine Receptor with Ligands: the Role of Gln117 and Other Residues of the Receptor in Agonist Binding. *J. Med. Chem.* **2008**, *51*, 6293–6302.

(50) Bisson, W. H.; Westera, G.; Schubiger, P. A.; Scapozza, L. Homology Modeling and Dynamics of the Extracellular Domain of Rat and Human Neuronal Nicotinic Acetylcholine Receptor Subtypes Alpha4beta2 and Alpha7. *J. Mol. Model.* **2008**, *14*, 891–899.

(51) Ulens, C.; Akdemir, A.; Jongejan, A.; van Elk, R.; Bertrand, S.; Perrakis, A.; Leurs, R.; Smit, A. B.; Sixma, T. K.; Bertrand, D; de Esch, I. J. Use of Acetylcholine Binding Protein in the Search for Novel Alpha7 Nicotinic Receptor Ligands: *in silico* Docking, Pharmacological Screening, and X-ray Analysis. *J. Med. Chem.* **2009**, *52*, 2372–2383.

(52) Sander, T.; Bruun, A. T.; Balle, T. Docking to flexible nicotinic acetylcholine receptors: A Validation Study Using the Acetylcholine Binding Protein. *J. Mol. Graphics Modell.* **2010**, *29*, 415–424.

(53) Xiu, X.; Puskar, N. L.; Shanata, J. A. P.; Lester, H. A.; Dougherty, D. A. Nicotine Binding to Brain Receptors Requires a Strong Cation-π Interaction. *Nature* **2009**, *458*, 534–537.

(54) Blum, A. P.; Lester, H. A.; Dougherty, D. A. Nicotinic pharmacophore: The Pyridine N of Nicotine and Carbonyl of Acetylcholine Hydrogen Bond across a Subunit Interface to a Backbone NH. *Proc. Natl. Acad. Sci. U.S.A.* **2010**, *107*, 13206–13211.

(55) Puskar, N. L.; Xiu, X.; Lester, H. A.; Dougherty, D. A. Two Neuronal Nicotinic Acetylcholine Receptors - $\alpha 4\beta 4$ and $\alpha 7$ Show Differential Agonist Binding Modes. *J. Biol. Chem.* **2011**, *286*, 14618−14627.

(56) Tonder, J. E.; Hansen, J. B.; Begtrup, M.; Pettersson, I; Rimvall, K.; Christensen, B.; Ehrbar, U. lessen, P. H. Improving the Nicotinic Pharmacophore with Series of (Isoxazole)methylene-1-azacyclic Compounds: Synthesis, Structure-Activity Relationship, and Molecular Modeling. *J. Med. Chem.* **1999**, *42*, 4970−4980.

(57) Hibbs, R. E.; Sulzenbacher, G.; Shi, J.; Talley, T. T.; Conrod, S.; Kem, W. R.; Taylor, P.; Marchot, P; Bourne, Y. Structural Determinants for Interaction of Partial Agonists with Acetylcholine Binding Protein and Neuronal $\alpha 7$ Nicotinic Acetylcholine Receptor. *EMBO J.* **2009**, *28*, 3040−3051.

(58) Bodnar, A. L.; Cortes-Burgos, L. A.; Cook, K. K.; Dinh, D. M.; Groppi, V. E.; Hajos, M.; Higdon, N. R.; Hoffmann, W. E.; Hurst, R. S.; Myers, J. K.; Rogers, B. N.; Wall, T. M.; Wolfe, M. L.; Wong, E. Discovery and Structure-Activity Relationship of Quinuclidine Benzamides as Agonists of $\alpha 7$ Nicotinic Acetylcholine Receptor. *J. Med. Chem.* **2005**, *48*, 905−908.

(59) Breining, S. R.; Bencherif, M.; Grady, S. R.; Whiteaker, P.; Marks, M.; Wageman, C. R.; Lester, H. A.; Yohannes, D. Evaluation of Structurally Diverse Neuronal Nicotinic Receptor Ligands for Selectivity at Alpha6* Subtype. *Bioorg. Med. Chem. Lett.* **2009**, *19*, 4359−4363.

(60) Unwin, N. Refined Structure of the Nicotinic Acetylcholine Receptor at 4 Å Resolution. *J. Mol. Biol.* **2005**, *24*, 1412−1522.

(61) Mazurov, A.; Hauser, T.; Miller, C. H. Selective $\alpha 7$ Nicotinic Acetylcholine Receptor Ligands. *Curr. Med. Chem.* **2006**, *13*, 1567−1584.

J

dx.doi.org/10.1021/ci3001953 | *J. Chem. Inf. Model.* XXXX, XXX, XXX−XXX